ASSESSMENT OF GRAVELLING IMPACT PHENOMENON ON HELICOPTER GLASS WINDSHIELDS

Gildas Langevin, gildas.langevin@airbus.com, Airbus Helicopters / Université de Rennes 1 (France)
Adrien Perret, adrien.perret@airbus.com, Airbus Helicopters (France)
Jean-Christophe Sangleboeuf, jean-christophe.sangleboeuf@univ-rennes1.fr, Université de Rennes 1 (France)
Ludovic Charleux, ludovic.charleux@univ-smb.fr, Université Savoie Mont Blanc (France)
Ulrich Eberth, ulrich.eberth@airbus.com, Airbus Helicopters (Germany)

Abstract

Gravelling is a critical topic on helicopter windshields, which consists of small particles impacting the front glazings during take-off and landing. A series of gravel-impacted spots have been selected on various windshields and analysed in order to pin potential influence factors, linked to the projectile and the impact conditions. Various tests have been performed so as to converge on a representative projectile which eventually allows reproducing the phenomenon in lab conditions. Typical impact conditions, and the alterations they induce, have thus been established. Finally, numerical models are detailed, with the aim of determining the respective influence of various damage characteristics dimensions on the residual strength of the sample

1. CONTEXT

1.1. Definition of gravelling

Helicopter windshields may suffer from various kinds of in-service damage.

In the one hand, birdstrikes usually lead to the windshield wreck, which explains why heavy helicopters regulations [1][2] require a bird impact resistance test, to ensure a safe landing. As a consequence, a bilayer technology made of an inner polymeric ply and an outer chemically toughened glass ply, is used on the corresponding windshields instead of single-layer polycarbonate or polymethylmethacrylate.
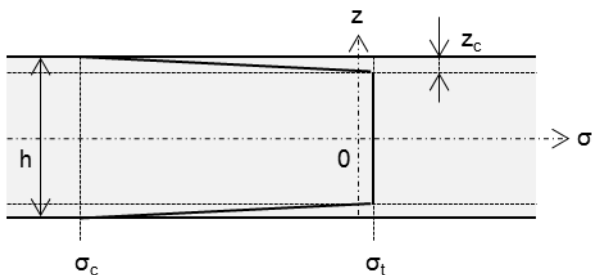

Figure 1 – Stress profile $\sigma_{ct}(z)$ created by chemical tempering: glass thickness h, compression layer depth z_c, superficial compression σ_c, residual core tension σ_t.

The glass layer is toughened by an ionic exchange process called chemical tempering, which stress profile and process are respectively shown in Figure 1 and Figure 2, creating a superficial compression layer hence improving scratch and impact resistance.
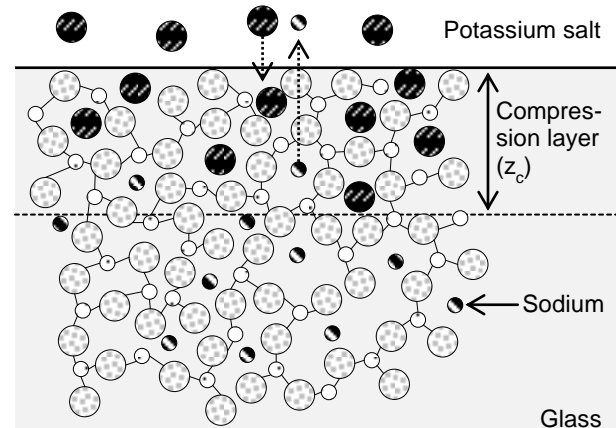

Figure 2 – Chemical tempering process: ionic exchange between potassium and sodium.

On the other hand, the air flow generated by the blades during take-off or landing is powerful enough to create a cloud of small particles originating from the ground, called brownout [3][4]. The main concern raised in this case is about visibility; however, lots of airborne particles possibly impact the windshields.

Gravelling stands in-between, both in terms of particle size and potential criticality for the windshield integrity. Due to the inherent brittleness of the glass, macroscopic cracks occur along windshields, often going through small superficial damage created by gravel impacts. This phenomenon is highly variable

from a windshield to another, in terms of damage quantity, size and repartition.

1.2. Description of the current test protocol

The performance of a potential transparent windshield material towards gravelling is currently a two-step process: a 1.6mm-wide steel ball impact test is performed first, in order to damage the sample. The post-impact alterations of the sample are then evaluated through a four-point flexural test.

This protocol is very repeatable since the projectiles are standardized roller bearings balls. Nevertheless, two main flaws limit the quality of the results. First, the impact produces a very specific damage physiognomy shown in Figure 3 called a hertzian crack [6], which representativeness is not ensured.
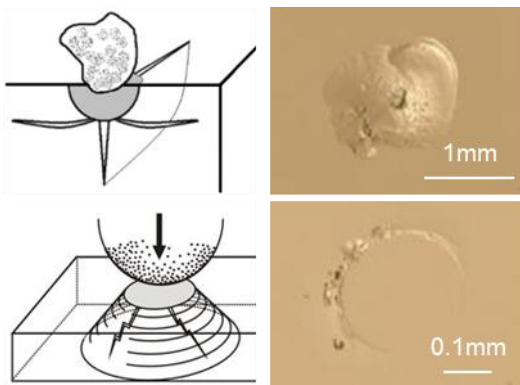

Figure 3 – Generic damage patterns created by a particle impact (*top*) (drawing from [5]); hertzian cone crack generated by the current steel ball test (*bottom*).

The second limitation appears during the flexural test: in case of light impact damage, the sample failure initiates at its edge, because the cutting process generates bigger defects than the impact itself. This means that slight mechanical alterations cannot be assessed through this process.

1.3. Problematics

The concern about hertzian cone cracks representativeness comes mainly from a lack of understanding of actual gravelling impacts: their damage profiles and patterns, as well as the potential damage criticality factors are suspected although not known exactly.

Consequently, a comprehensive study of actual gravelling impacts seems like a natural first step, before trying to reproduce them in lab conditions.

2. IN-SERVICE IMPACTS ANALYSIS

2.1. Protocol

Several windshields have been collected; coming from various helicopter models (NH90, H225),

places (Japan, Sahel Desert and southern France), and locations on the canopy (left, central when applies, and right). Damage spots have been selected, in order to elaborate a damage database.

Samples are then extracted, and profilometric scans of the damaged spots are made. They show typical spalling patterns already seen in the literature and displayed in Figure 3 (top).

Various geometric quantities (see Figure 4) are measured on each impact, namely:

- The maximal superficial damage depth: z_{max},
- The diameter of the circle inscribed in the spalled area: d_{min},
- The diameter of the circle circumscribing the spalled area: d_{max},
- The diameter of the shattered area: d_{impact}.

A "roundness factor" noted R (1), is then defined as the ratio between the area of the inscribed and circumscribing circles, in order to evaluate the axial symmetry of the spalling patterns.

$$(1) \quad R = \left(\frac{d_{min}}{d_{max}} \right)^2$$
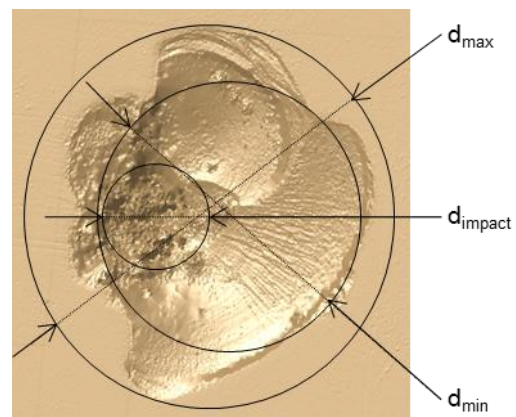
R is expressed as a percentage.

Figure 4 – Geometric data measured on a damaged area.

2.2. Evidence of material-related damage factors

Central windshields have been compared in Figure 5 below.

In spite of important dispersions, Figure 5 shows some significant variations between the Japanese helicopter and the two others. Considering the air flows approximately identically around those central windshields, the variations observed highlight the influence of possible projectile-related damage factors such as their shape, weight/density, and hardness.
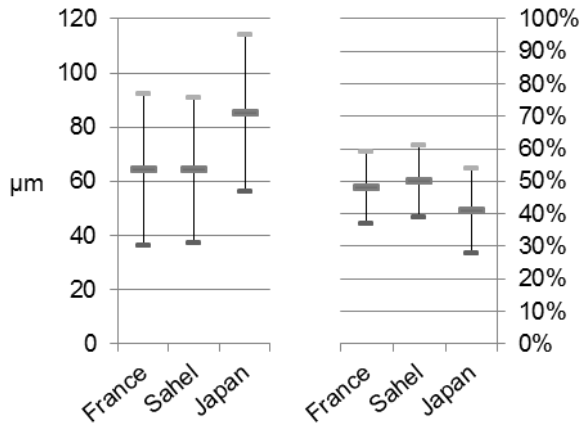
Figure 5 – Comparison of central windshields: z_{max} (*left*) and R (*right*).

2.3. Evidence of impact-conditions damage factors

The Japanese windshields also have been compared: they have been extracted from the same helicopter, thus provide a reliable way to evaluate possible impact-conditions-related damage factors, as shown in Figure 6.
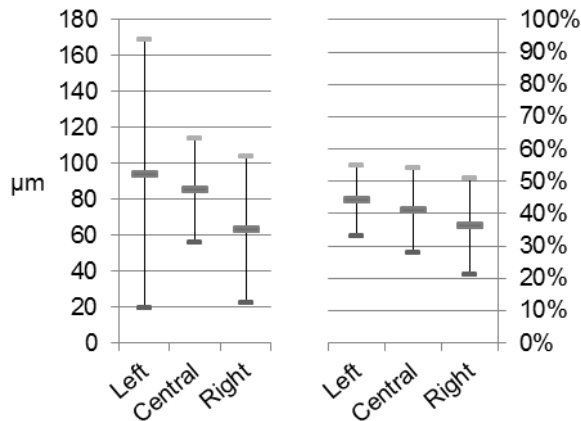

Figure 6 – Comparison of Japanese helicopter windshields: z_{max} (*left*) and R (*right*).

The evolution from left to right is significant, although biased by high dispersions: the superficial damage depth and the roundness ratio both decrease, meaning the impacts create less intense, less asymmetric damage. This could indeed highlight the importance of impact conditions, namely projectile velocity and incidence angle.

This preliminary step shows several possible damage criticality influence factors, related to the projectile itself as well as the impact conditions. Environmental factors should be considered too, given that windshields should survive various temperature and moisture conditions [7] at which glasses damage extension may evolve [8].

Their respective influences need to be studied in order to elaborate a representative gravelling test protocol.

3. DEFINITION OF A REPRESENTATIVE TEST PROTOCOL

3.1. Preliminary: determination of valid environmental conditions

3.1.1. Experimental setup

The objective of this preliminary step is to evaluate the behavior of the windshield glass layer under various environmental conditions. Given that the -55°C – 85°C ground survival temperature range mentioned in [7] is well under the estimated 500°C glass transition temperature [9], the impact response of the glass is not supposed to show any significant variations. However, the damaged glass post-impact behavior is expected to change depending on its environment, namely by crack growth.

This damage evolution preferentially occurs inside the core material and not in the chemically tempered, compressed surface layer. For this reason, and due to material availability and cost concerns, this step is realized on standard soda-lime silica glass: SEM analyses have shown an identical composition to the core windshield glass.

Several Vickers indentation loads have been realized, in order to select a preliminary damaging process. About 15 minutes after indenting the samples, an equibiaxial flexural test is performed following ASTM C1499 recommendations [10] so as to evaluate the post-damage residual strength of the sample while avoiding edge effects.

Figure 7 below shows the typical statistical behavior of intact glass: failure can happen on a very wide range of applied loads, depending on the surface microscopic state of the material in the loaded area.
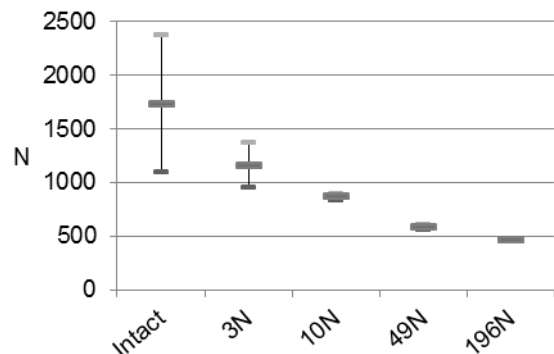

Figure 7 – Evolution of equibiaxial flexural failure load with indentation load.

The material failure becomes deterministic from 10N indentation damage. Practically, the 196N indents

are chosen, because they all feature fully developed median-radial and lateral cracks patterns.

3.1.2. Results

3.1.2.1. Humidity variation

The damage evolution with time and humidity have been observed. The test samples have been stored for various durations in two different atmospheres: a first batch in a controlled 20°C, 50%RH lab room, and a second one in a 20°C, saturated environment.

The failure strength evolutions are displayed in Figure 8 below, where 100% is the reference value obtained with standard 196N identations.
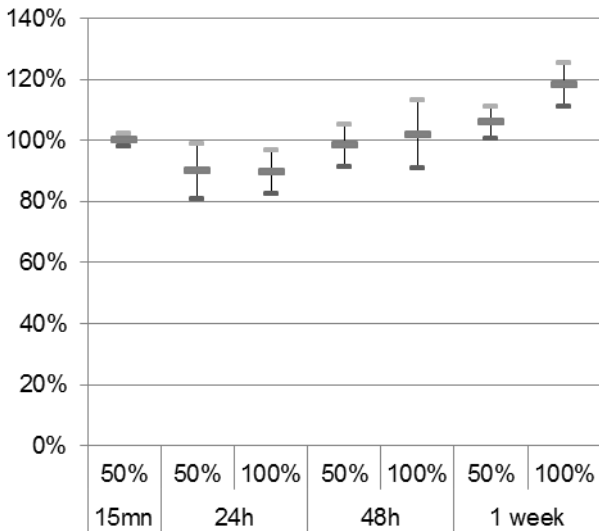

Figure 8 – Evolution of relative failure load with storage time and moisture.

In every case, a saturated humidity level seems to have an attenuating effect on the damage criticality; this cannot be explained yet, because such a "healing" effect only has been observed at much higher temperature [11].

The effect of storage duration is not clearly understood either: while a 24h storage leads to a strength decrease that can be explained by subcritical crack propagation [8], the strength increase observed afterwards, over the reference value, has no explanation from the literature.

These results must be qualified by the increased dispersions. However, the strength variations do not exceed 10% of the reference value, to be taken into account for future impact damage analyses.

3.1.2.2. Temperature variation

This step focuses on the role of temperature. The samples batches have been stored at room temperature, 85°C and -7.5°C respectively. After the storage duration, the samples are put back to room temperature before proceeding to the equibiaxial flexural test. The results are shown in Figure 9.
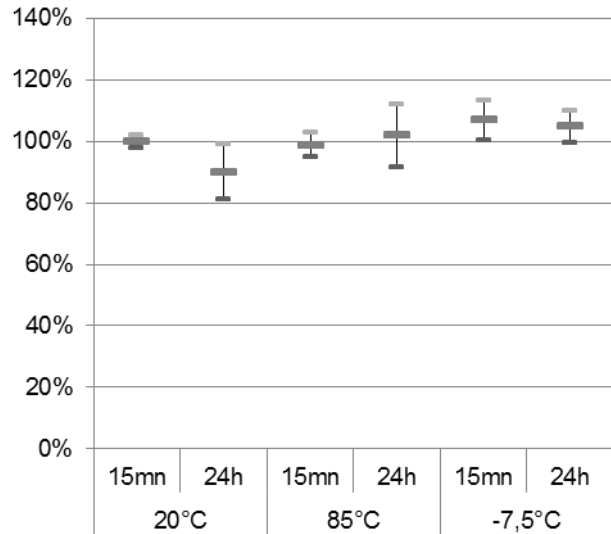

Figure 9 – Evolution of relative failure load with storage time and temperature.

Whatever the storage duration is, high temperature appears to have a very light aggravating effect, whereas cold storage induces an improved damage strength.

3.1.2.3. Thermal cycles

The role of thermal cycles has also been studied. The samples have switched between 15mn/24h cold and hot storage with transition periods shorter than 10s, in order to highlight possible thermal shock effect on the indents. The results are shown in Figure 10.
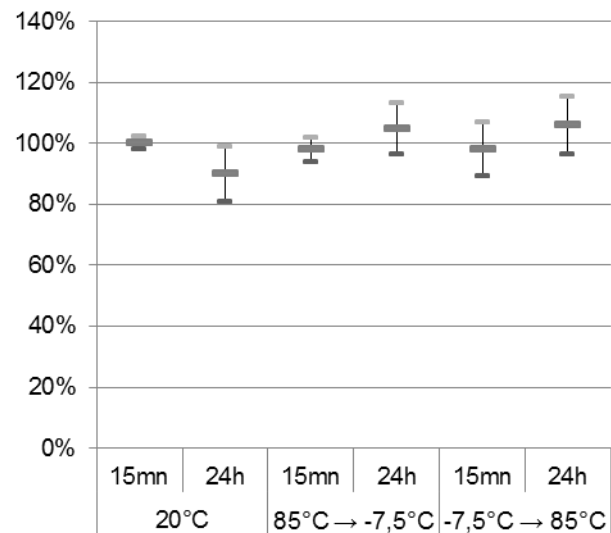

Figure 10 – Variation of relative failure load with several thermal cycles.

The effect of 15mn cycles seems limited, compared with their 24h equivalent which show higher variation yet decreased indent damage criticality.

The environmental conditions induce variations both

above and beyond the reference lab atmosphere results which, given its average criticality, should be considered valid and representative for further tests.

3.2. Selection of a projectile

3.2.1. Objectives and experimental setup

The aim on this second step is to converge on a projectile that should be representative of a piece of gravel, yet standardized enough to allow the definition of a standardized gravelling test set-up to be added in new windshield specifications.

Several materials, shapes and weight are successively tested and selected in function of the damaging topology they create at given impact conditions. This step focuses on the material impact response and therefore, the standard soda-lime silica glass cannot be used anymore, since it is not toughened.

For windshield glass availability reasons, another sample material needs to be used: these tests are performed on another chemically tempered soda-lime silica glass. Its composition is identical to both the windshield glass and the standard equivalent used in 3.1, and it is tempered following the same ionic exchange process between sodium and potassium, which gives them comparable Vickers hardness values. The only difference between this glass and its windshield equivalent are the superficial compression value (400MPa instead of 300MPa) and layer depth (20µm instead of 70µm).

The test protocol is a two-phase process: an impact test is performed, where the projectile is thrown onto the sample with an air gun (see Figure 12). Following the impact, the equibiaxial flexural test is performed in order to quantify the strength alterations created by the impact.

3.2.2. Material selection

A preselection of materials is made first, following several criteria.

They must be rocky, so as to feature gravel-representative macroscopic granularity and hardness. The risk using other materials, such as metals or ceramics, is to overestimate the criticality of the impact conditions tested: such projectiles would probably transfer all their kinetic energy to the glass because of their higher hardness and rigidity, instead of shattering on impact.

From a practical standpoint, the projectile materials must be commercialy available for repeatability purposes, as well as easy to machine/cut with laboratory devices.

Eventually, three materials are preselected in order to make representative projectile: limestone, quartzite and flint. They fulfill all the requirement detailed above, and cover a wide range of Vickers hardnesses.

Identical projectiles, 1g, square-based-pyramid shaped are made out of these rocks, and thrown on glass sample at normal incidence and various velocities (see Figure 12). The results of the equibiaxial flexural tests are shown in Figure 11 below, where 100% is the strength of the intact glass.

The material choice is eventually made by eliminations. The flint impactors are too critical for further use, because they tend to totally break the glass sample on impact, which practically happens very rarely on windshields.
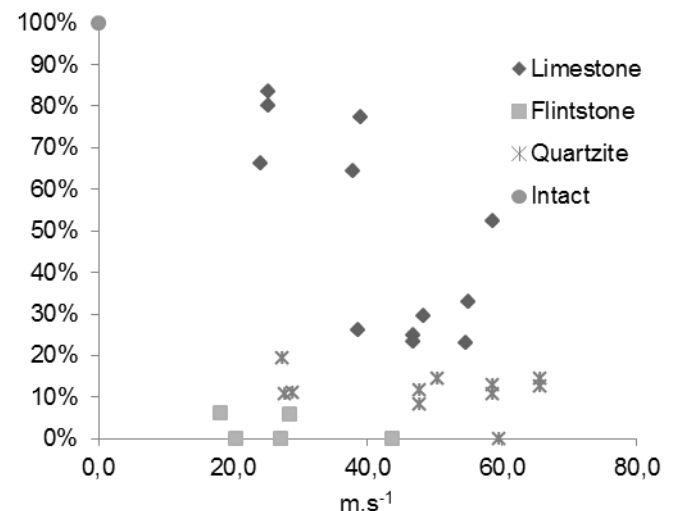
Figure 11 – Evolution of the residual mechanical strength of the glass, in function of the projectile velocity.

Limestone seems to give interesting results, with a wide variety of impact criticality values. However, rock particles very often remain stuck inside the damage, which prevents any possible damage geometric measurements and thus any comparison with the actual impacts studied in 2.

Quartzite is consequently elected as projectile material: it offers a wide range of possible impact velocities, and allows a good damage visibility. The alterations it creates on 20µm-tempered glass are rather important, but the switch to 70µm-tempered windshield glass and lower incidence angles are expected to give a wider range of alterations.
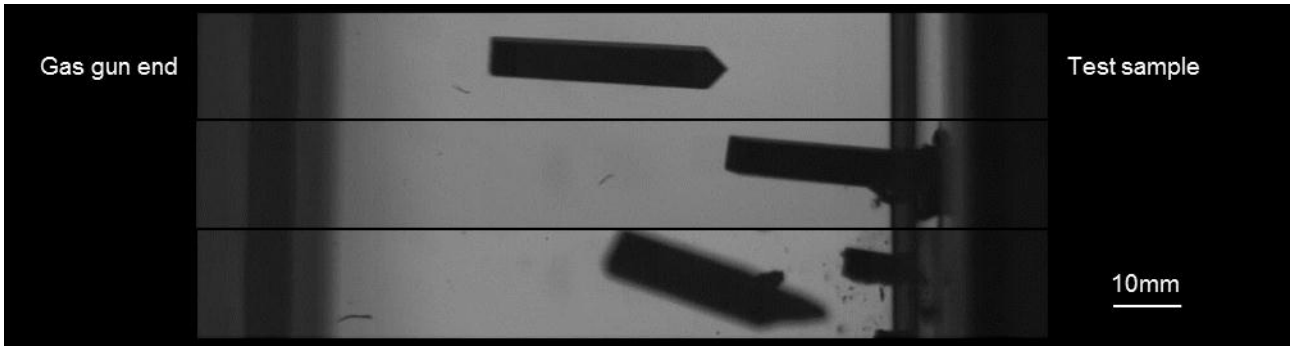
Figure 12 – Three consecutive screenshots of a damage generation.

3.2.3. Shape selection

Three projectiles tip shapes are preselected: Vickers indenter, cube corner and square-based pyramid. However, the first option is practically not feasible: the angle of a Vickers indenter (136°) is very wide, and the air gun used for the impact tests does not provide a good enough trajectory control to allow enough conform shots.

Cube corner and pyramidal projectiles are built with controlled tip radius and deviations, so as to quantify their geometry and ensure reproducibility. They are thrown at various velocities on the 20µm glass. The results of the equibiaxial flexure are shown below.
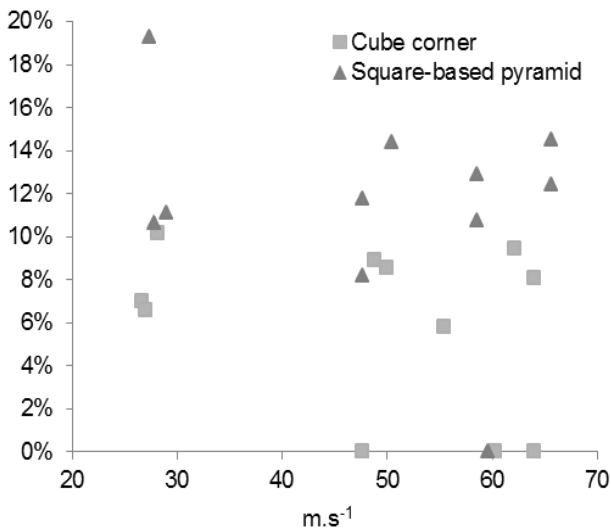

Figure 13 – Evolution of residual mechanical strength of the 20µm tempered glass, in function of the projectile velocity.

The cube-corner-shaped projectiles prove to be slightly more critical than the pyramidal ones in terms of sample residual strength, and cover the same range of velocities. Due to easier and less time-consuming building process, this geometry is chosen for the projectile shape.

3.2.4. Mass determination

The mass of the projectile has previously been identified as a possible impact criticality factor. As a first approximation, a range of possible gravel stone masses have been estimated from 0.5g to a few grams, thanks to airfield aggregates sieve sizes [12] and measured gravel densities.

As a consequence, a series of iso-kinetic-energy impact tests has been performed with various quartzite projectile masses, as shown in Figure 14 below.
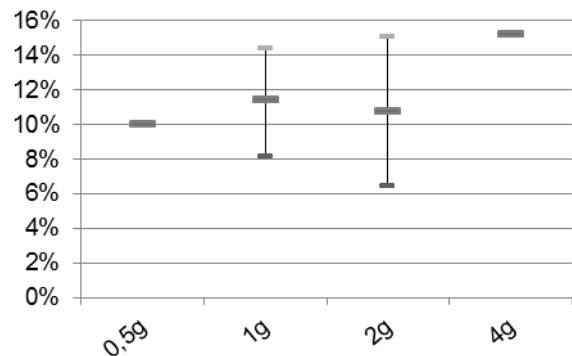

Figure 14 – Alterations generated by 1J (± 20%) impacts at various masses.

The 0.5g and 4g projectiles shots are difficult to realize: the former ones suffer from important trajectory deviations while the latter ones often lead the glass sample to break from its edge. In both cases, only one valid test has been performed, which explains the absence of error bars in Figure 14.

No significant variations have been observed between 1g and 2g impacts alterations, except slightly increased dispersions in the latter case.

For manufacturing convenience reasons, 1g projectiles are chosen for further tests.

4. ASSESSMENT OF IMPACT CONDITIONS INFLUENCE

4.1. Objectives and experimental setup

At the end of the previous step, a 1g cube-corner quartzite is chosen to reproduce gravel impact,

which from now on is used to assess the influence of impact conditions, namely velocity and incidence angle.

The aim is now to reproduce typical gravel impact conditions as closely as possible so that real-life damage can be linked to impact conditions. This means the 70µm-tempered windshield glass has to be used.

As before, the samples are damaged thanks to air gun shots; the damage-induced alterations are then quantified through equibiaxial flexural tests.

4.2. Results

The incidence angle is defined as shown in Figure 15 below. Several values are tested: normal (90°), quasi-normal (70°), medium inclined (45°) and grazing incidence (20°).
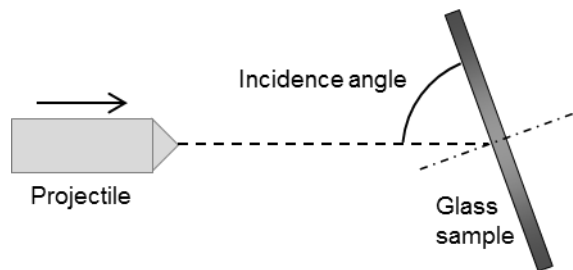
Figure 15 – Incidence angle definition

This parameter seems to act as a multiplication factor: medium and grazing incidence allow to obtain higher velocity. This is why Figure 16 only shows the evolution of the damage criticality with the normal component of the velocity vector instead of its norm.

The alterations generated by impact can be separated in two types: a few ones can be considered "light", when the sample maintains between 50% and 80% of its intact strength, while most of them are significant, only maintaining fewer than 30% of the intact strength.
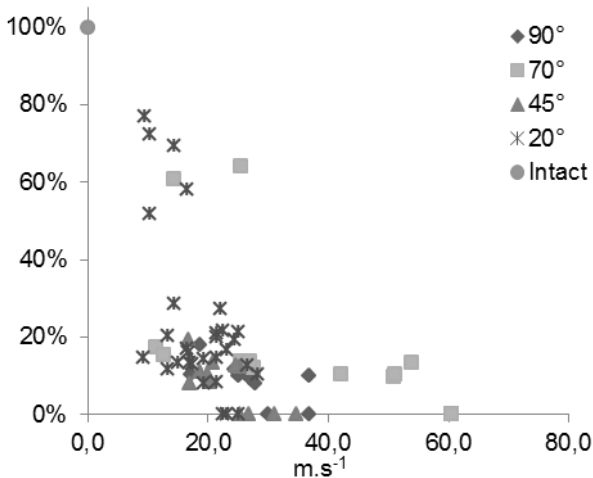
Figure 16 – Evolution of impacted area residual strength with normal velocity at various incidences.

The geometric data shows a notable result: the dependency between the residual strength of the sample and the visible damage depth (when observed from the surface) appears much more clearly, as seen in Figure 17 below.

The gap between light and significant damage highlighted above can be explained by its depth: a light alteration corresponds to a very superficial damage (under 25µm, as seen from the surface), and a significant one is more than 25µm deep.
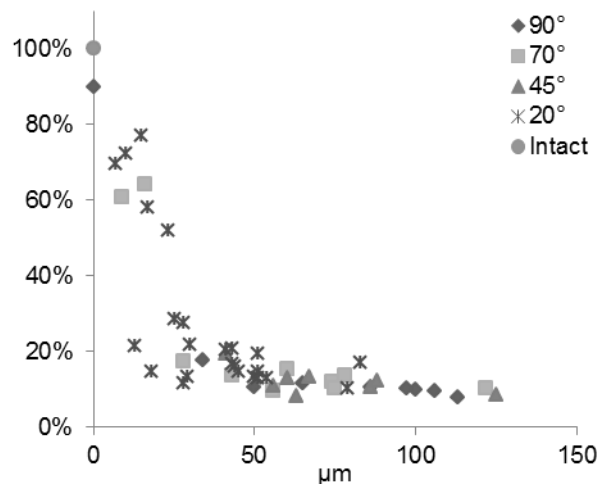
Figure 17 – Evolution of damaged area residual strength with superficial damage depth.

4.3. Analytical model

Being able to model analytically the evolution of strength alterations with superficial depth can be a good complement, in order to understand the physics of these alterations and consequently predict more accurately future damage.

4.3.1. Actual damage depth estimation

The first step is to predict the damage depth, from what is visible from the surface to the actual value. Vickers indentation tests have been performed on windshield tempered glass at 49.03N, 98.07N and then 196.1N. The samples then have been broken, in order to get a lateral view of the damage, from an edge: the depths of the central shattered area and the global damage have been measured and compared:

$$(2) \quad \frac{z_{total}}{z_{multifissuration}} = 2.74 \pm 3\%$$

4.3.2. Erosion model

In this first model, the damage spot is considered "flat enough" so that no stress concentration appears, which can be interpreted as if the damaged area was showing by local erosion on a depth z_{max}.

Following Figure 1 notations and ASTM C1499

formulas [10], the sample failure stress σ_f is defined as:

$$(3) \quad \sigma_f\left(z = -\frac{h}{2}\right) = \beta.\frac{F_{max}}{h^2}$$

Where β is a coefficient defined in [10], which depends on the geometry of the equibiaxial flexural test (dimensions of the sample, of the support and loading rings) and the Poisson ratio of the glass.

Since the damage has a depth z_{max}, the stress state at the damage tip is defined by the Strength of Materials theory as:

$$(4) \quad \sigma_f\left(z = -\frac{h}{2} + z_{max}\right) = \beta.\frac{F_{max}}{h^2}.\left(\frac{-\frac{h}{2} + z_{max}}{-\frac{h}{2}}\right)$$

If the intrinsic failure stress of the glass σ_{int} is considered uniform in the material:

$$(5) \quad \sigma_f(z) + \sigma_{ct}(z) = \sigma_{int} \forall z \in \left[-\frac{h}{2};+\frac{h}{2}\right]$$

Where $\sigma_{ct}(z)$ is the chemical tempering stress profile displayed in Figure 1, then $F_{max}(z_{max})$ can be evaluated combining (4) and (5) as such:

$$(6) \quad F_{max} = \frac{h^3}{\beta.(h - 2.z_{max})}\left[\sigma_{int} - \sigma_{ct}\left(-\frac{h}{2} + z_{max}\right)\right]$$

4.3.3. Graphic comparison

The estimated damage depth has been extrapolated from Figure 17 and (2), and superposed with a plot of (6) in Figure 18 below.
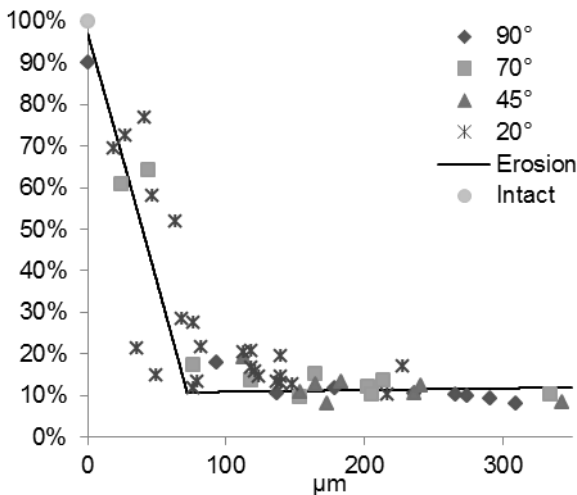

Figure 18 – Evolution of damaged area residual strength with estimated actual damage depth: superposition of experimental data and analytical model.

The analytical erosion model seems to show a good correlation with the adapted experimental data. As a consequence, it can be used for further chemically tempered glasses comparisons, since they only require manufacturer/literature data and a few sample indentations.

4.4. Comparison with steel ball impact test

An improved steel ball test protocol has been established, adding incidence variation to the impact conditions and replacing the former four-point-flexural by an equibiaxial on. The objective is to check the relevance of the steel ball as a projectile, compared with the more realistic, less standardized quartzite cube corner.

There is a much more important gap between light and critical damage than with quartzite cube corners, which is however linked again to the maximal visible depth as shown in Figure 19 below.
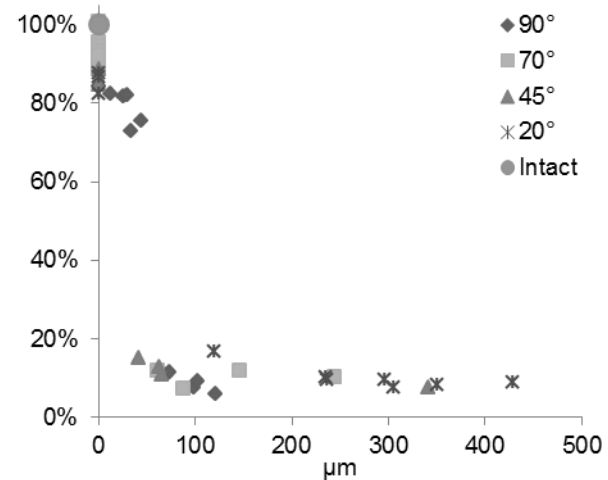

Figure 19 – Evolution of damage criticality with superficial damage depth, for steel ball impact tests.

4.5. Experimental conclusions

This step has permitted a refined understanding of sample-scale windshield upon impact. A wide set of impact conditions has been tested, and the damage obtained covers the same range of superficial depth as what has been observed on windshields in 2.2 and 2.3.

More specifically, the maximal visible depth proves to be a good criticality indicator. This is, practically, very important, because this can now be used as a non-destructive diagnostic tool for future applications: for instance, if a helicopter comes back with damaged windshields from a flight, a surface analysis with nanometric paste or a portable profilometer can be made in order to estimate the probability of future macroscopic crack initiation, within a few minutes.

Finally, the relevance of the steel ball as a gravel-like projectile has shown some limitations. Its high degree of standardization means it can still be used to compare several windshield solutions, unfortunately with a narrower range of possible alterations.

5. NUMERICAL COMPARISON

5.1. Objectives

Numerical models have been developed in parallel, with two main goals: firstly, to confirm the experimental results and being able to model any kind of gravel damage that could occur; then, to be able to predict the behaviour of potential new windshield solutions after a given impact.

5.2. Description of the models

The models developed on this study aim to reproduce numerically the equibiaxial flexural test. This is a quasi-static loading, which justifies the use of a finite-element implicit code, here ABAQUS/Standard [13]. The models are pre- and post-processed with Abapy [14] and Gmsh [15].

5.2.1. Geometry - mesh

The model is composed of the sample, as well as a support ring and a loading ring. Standard hard contacts are set up.

For computing cost concerns, this model is axisymmetric; since the actual samples previously used are squared, its radius has been adapted following ASTM C1499 square/disk equivalence [10].

The chemical-tempering-induced prestress profile has a high influence on the sample failure behaviour. Consequently, it has to be modelled. This explains significantly refined elements at both surfaces of the sample.
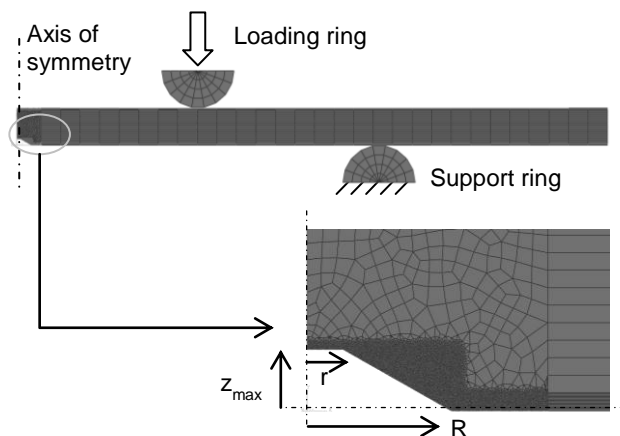

Figure 20 – General view of a model; detail on damage parameters.

The mesh has a hybrid formulation: indeed, hexaedral elements generally adapt better to the potential loads and are used in most of the sample as well as the rings. Nevertheless, they cannot represent accurately enough a general damage, which is why the central refined box has been meshed with mixed tetrahedral/hexaedral elements

Axisymmetric solid elements have been used, so that various kinds of damage geometry can be modelled if needed.

5.2.2. Material properties

All the components are modelled as purely elastic materials: indeed, the glass is brittle, thus can be considered macroscopically elastic until it breaks, whereas the rings are made of steel and considered rigid by hypothesis of the equibiaxial flexure test.

A failure criterion is set to σ_{int} (see (5)) to the glass sample during postprocessing, based on the maximal principal stress on the surfaces.

5.2.3. Boundary conditions, loads

As mentioned before, symmetry conditions have been entered to gain computation time. The chemical tempering stress profile is modelled via a predefined field. The support ring is totally fixed, while the load ring is given a ramp vertical displacement condition.

5.2.4. Damage modelled

Several damage geometric parameters (shown in Figure 20 above) are modelled, matching with what has been measured in 2.1: z_{max} (damage depth), r (multifissuration radius) and R (spalling radius). A design of experiments has been set up so as to isolate the effects of these factors, as well as possible z/r or r/R cross-influences.

5.3. Results

5.3.1. Design of experiments

The design of experiments returns weightings shown in (7) below.

(7) confirms the primary importance of damage depth as a criticality indicator, whereas all the other parameters as well as their cross-influences are negligible.

$$
\begin{aligned}
F_{failure}(\%) = {}& 41.60 \\
& + \begin{bmatrix} +54.7 & +48.56 & +32.06 \\ +4.53 & -21.58 & -24.67 \\ -27.12 & -32.95 & -33.56 \end{bmatrix} z \\
& + \begin{bmatrix} 0.00 & +0.22 & -0.22 \end{bmatrix} r \\
& + \begin{bmatrix} +0.40 & +0.01 & -0.41 \end{bmatrix} R \\
& + \begin{bmatrix} +0.44 & -0.10 & -0.34 \\ +0.53 & -0.32 & -0.21 \\ -0.97 & +0.42 & +0.55 \end{bmatrix} r.R \\
& + \begin{bmatrix} +0.36 & +0.15 & -0.51 \\ 0.00 & -0.22 & +0.22 \\ -0.35 & +0.47 & -0.12 \\ +0.32 & +0.10 & -0.42 \\ 0.00 & -0.22 & +0.22 \\ +0.30 & +0.09 & -0.39 \\ -0.01 & -0.23 & +0.24 \\ -0.61 & +0.09 & +0.53 \\ 0.00 & -0.22 & +0.22 \end{bmatrix} z.r
\end{aligned}
\qquad (7)
$$

5.3.2. Numerical – experimental comparison

The evolution of the numerically-obtained residual mechanical strength with depth has also been studied for a constant spalling radius of 0.8mm, which is an average value determined from in-service impact analysis. The results are plotted and compared with the experimental data in Figure 21 below.

These numerical models fit correctly the experimental data, which means they can be used for further chemically tempered glasses comparisons.
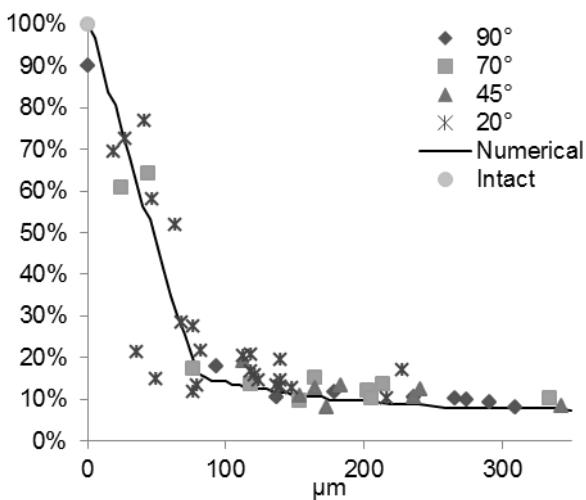

Figure 21 – Evolution of damaged area residual strength with estimated actual damage depth: superposition of experimental data and analytical model.

6. CONCLUSIONS – PROSPECTS

A comprehensive study of gravelling impacts on helicopter windshields has been lead from the natural starting point that is the analysis of damaged windshields, to their reproduction both experimentally and numerically at sample-scale.

The convergence towards a representative projectile gives the chance to quantify more accurately the response of future prototype windshields to gravel impacts.

Finally, the discovery of the surface damage depth as a non-destructive impact criticality assessment now gives the possibility to predict the maximal load a windshield can withstand before breaking due to a crack. The numerical simulations have confirmed the relevance of this parameter.

There are still potential improvements to be found though. The test protocol presented has been standardized as much as possible with the available material; however an already existing impact device might turn out to give more efficient windshield comparisons in the long term.

The next step consists in studying the damage environment, in other words expanding to a full windshield scale. This should allow a better understanding of what kinds of loads a damaged area can be submitted to, and eventually give a comprehensive view of the phenomenon of gravelling.

7. REFERENCES

[1] European Aviation Safety Agency. *CS-29 – Certification Specifications for Large Rotorcraft*

[2] Federal Aviation Administration. *Federal Aviation Regulations*, Part 29 – Airworthiness Standards: Transport Category Rotorcrafts

[3] JASION, G.T. *Toward a physics based entrainment model for simulation of helicopter brownout.* University of Southampton PhD Thesis, 2013

[4] JOHNSON, B., LEISHMAN, J.G., SYDNEY, A. Investigation of Sediment Entrainment Using Dual-Phase, High-Speed Particle Image Velocimetry. *Journal of the American Helicopter Society*, vol. 55, no 4, p. 42003-1-16, 2010.

[5] ISMAIL, J., ZAÏRI, F., NAÏT-ABDELAZIZ, M., et al. Experimental and numerical investigations on erosion damage in glass by impact of small-sized particles. *Wear*, vol.271, no 5, p. 817-826, 2011.

[6] JOHNSON, K.L. One hundred years of Hertz contact. *Proceedings of the Institution of Mechanical Engineers,* 196(1), 363-378, 1982.

[7] EUROCAE ED-14G (RTCA DO-160G): Environmental conditions and test procedures for airborne equipment

[8] FREIMAN, S.W., WIEDERHORN, S.M., MECHOLSKY J.R. Environmentally enhanced fracture of glass: a historical perspective. *Journal of the American Ceramic Society*, vol. 92, no 7, p. 1371-1382, 2009.

[9] BARTON, J., GUILLEMET, C. *Le verre*. Science et Technologie, 2005

[10] ASTM C1499-15. *Standard Test Method for Monotonic Equibiaxial Flexural Strength of Advanced Ceramics at Ambient Temperature*

[11] WILSON, B.A., CASE, E.D. Effect of humidity on crack healing in glass from in-situ investigations using an ESEM. *Journal of materials science*, 1999, vol. 34, no 2, p. 247-250.

[12] AFNOR. *EN13043-2003 – Aggregates for bituminous mixtures and surface treatments for roads, airfields and other trafficked areas*

[13] http://www.3ds.com/products-services/simulia/products/abaqus/latest-release/

[14] https://zenodo.org/record/17784

[15] GEUZAINE, C., REMACLE, J.-F. Gmsh: A 3-D finite element mesh generator with built-in pre-and post-processing facilities. *International Journal for Numerical Methods in Engineering*, 2009, vol. 79, no 11, p. 1309-1331.

.